Self-Assembly and Characterisation of Grid-Type Iron(II), Cobalt(II) and Zinc(II) Complexes

Violetta Patroniak,[a,b] Paul N. W. Baxter,[a,d] Jean-Marie Lehn,*[a] Maciej Kubicki,[b] Maija Nissinen,[c] and Kari Rissanen[c]

Keywords: Grid-type complexes / Iron / Cobalt / Zinc / Supramolecular chemistry / Self-assembly

The reaction of the ligands **5** and **6**, containing two tridentate binding units, with iron(II), cobalt(II) and zinc(II) leads to the self-assembly of supramolecular architectures of [2 × 2] grid type containing four ions in octahedral coordination sites. The grid-type structures have been assigned on the basis of the spectroscopic data in solution, and confirmed in the solid state in the case of complexes **6b** and **6c** by X-ray crystallography. The latter study revealed that each metal ion is situated in a distorted octahedral coordination environment comprising two N,N,O ligand donor sets.

Introduction

Self-assembly has been defined as the spontaneous but directed formation of a closed superstructure or polymer from a mixture of components (organic ligands, salt crystals, and sometimes molecules of solvents).[1] The product exhibits a notable thermodynamic and kinetic stability and its components should contain all the information necessary for a correct assembly to occur. Self-assembly has recently been achieved in many types of organic and inorganic systems.[2] Inorganic self-assembly involves the spontaneous generation of well-defined metallo-supramolecular architectures from mixtures of organic ligands and metal ions. This latter approach has proven particularly successful for the generation of a wide spectrum of architectural types such as, for example, inorganic double and triple helicates,[1,3] rotaxanes,[4] clusters,[5] racks,[6] cages,[7] grids[8] etc., based on ligand design and on the application of suitable coordination geometries for the assembly process. Among them, there is an increasing interest in grid-shaped complexes, based on ligands containing oligopyridine-type groups and various transition metal ions. The grids are the thermodynamically most stable motif when metal ions of octahedral coordination geometry are combined with a linear ligand containing two tridentate binding subunits. Such compounds may exhibit novel physical (electronic,[8a] magnetic[8g−8i]) and chemical properties with potential applications in supramolecular engineering, nanotechnology, biomedical inorganic chemistry or biological catalysis. Transistors incorporating complexes containing a cobalt ion bonded to polypyridyl ligands have been reported recently, and this development is expected to be important in molecular electronics and in the study of the physics of nanoscale systems.[9]

In this paper we describe the syntheses, structural characterisation and luminescence properties of some polynuclear metal complexes prepared from hexadentate ligands **5** and **6** containing pyridine, pyrimidine, and carbonyl donor groups. The syntheses of the new ligands and their precursors have been achieved in good overall yield. The coordination chemical investigations of **5** and **6** with metal ions of preferred octahedral coordination geometry, such as Fe^{II}, Co^{II} and Zn^{II} revealed that the ligands are correctly preorganised for the assembly of tetranuclear grid-type complexes.

Results and Discussion

Synthesis of Ligands 5 and 6

We have designed heterotopic ligands **5** and **6**, which each possess two unusual N,N,O tridentate binding subunits for the complexation of ions of octahedral coordination geometry. Ligands **5** and **6** comprise heterocyclic pyrimidine and pyridine units synthesised as outlined in Scheme 1.

2-Methyl-6-(trimethylstannyl)pyridine **(1)** was obtained from 2-bromo-6-methylpyridine by a halogen/lithium ex-

[a] ISIS, Université Louis Pasteur,
8, Allée Gaspard Monge, BP 70028, 67083 Strasbourg, France
E-mail: lehn@isis.u-strasbg.fr
[b] Faculty of Chemistry, Adam Mickiewicz University,
Grunwaldzka 6, 60780 Poznań, Poland
[c] Department of Chemistry, University of Jyväskylä,
P. O. Box 35, 40351, Jyväskylä, Finland
[d] Current address: Institut Charles Sadron
6 Rue Boussingault, 67083 Strasbourg, France

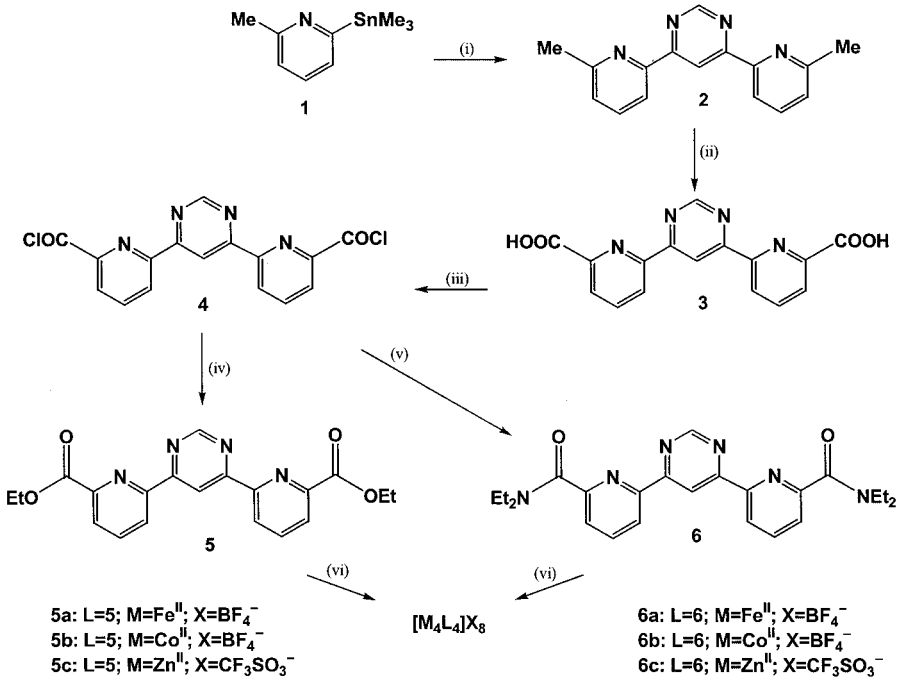

Scheme 1. Reaction scheme for the synthesis of the [2 × 2] grid complexes **5a**−**c** and **6a**−**c**. i) 4,6-dichloropyrimidine, LiCl, $Pd(PPh_3)_4$, toluene (90%), ii) H_2SO_4, CrO_3 (81%), iii) $SOCl_2$, iv) EtOH, (88%), v) Et_2NH, THF (38%), vi) $Fe(BF_4)_2$, $Co(BF_4)_2$ or $Zn(CF_3SO_3)_2$, CH_3CN

change protocol at low temperature in THF with *n*-butyllithium, followed by quenching the pyridyllithium intermediate with $ClSnMe_3$.[10] The twofold Stille-type[11] coupling reaction of **1** with 4,6-dichloropyrimidine in toluene using $[Pd(PPh_3)_4]$ as a catalyst furnished **2** in 90% yield after workup. The methyl groups of **2** were further oxidized with CrO_3 in concentrated H_2SO_4 to afford diacid **3** in 81% yield. The acid is insoluble in most organic solvents and only slightly soluble in DMSO. Precursor **3** was converted into the diacid dichloride **4** upon refluxing in $SOCl_2$. The diacid dichloride **4** was used subsequently in further transformations without purification. Thus, when **4** was refluxed with EtOH or stirred with Et_2NH in THF ligands **5** and **6** were obtained in 88% and 38% yields, respectively, after purification. The structures of **5**, **6** and precursors were confirmed by NMR spectroscopy, FAB-MS and elemental analysis. Ligands **5** and **6** were also structurally characterised by X-ray crystallography (Figure 1 and 2).

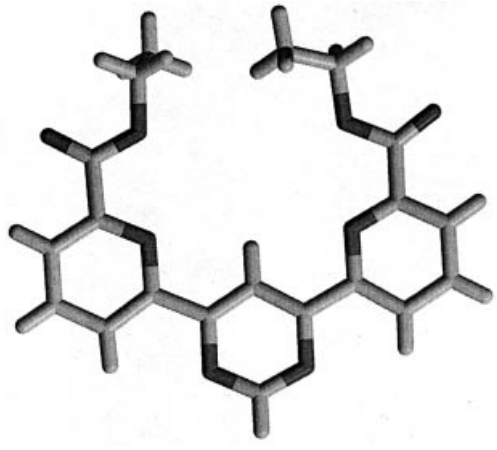

Figure 1. Single-crystal X-ray structure of ligand **5**

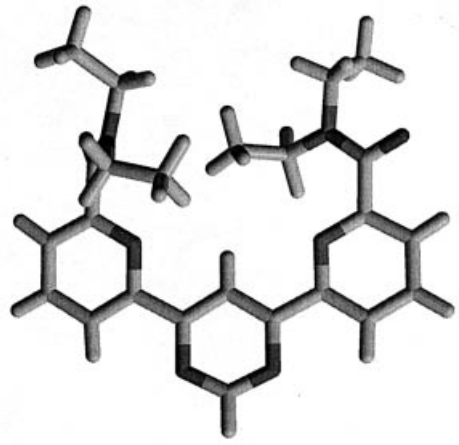

Figure 2. Single-crystal X-ray structure of ligand **6**

Both **5** and **6** exist in the solid state as *transoid* conformers (Figure 1 and 2) for N−C−C−N torsion angles (Table 1). This conformation is energetically favoured, as shown in earlier work.[12] It presents C−H···N intramolecular hydrogen bond interactions for further stabilisation (Table 2). However, in the metal complexes presented below the ligands exist in a *cisoid* conformation in which the terminal carbonyl oxygens form chelating coordination bonds with metal ions.

Table 1. Relevant torsion angles in the crystal structures of ligands **5** and **6**

	5A	5B	6
N1−C6−C7−N8	−178.9(5)	177.8(5)	−178.4(2)
N3−C4−C13−N14	177.6(5)	−179.9(5)	−169.7(2)
N14−C15−C19−O20	175.3(7)	178.0(6)	−119.5(2)
N8−C9−C24−O25	−172.8(6)	−172.6(7)	
N8−C9−C26−O27			−151.3(2)
C19−O21−C22−C23	159.9(7)	−98.0(7)	
C24−O26−C27−C28	97.6(7)	−162.3(6)	

The aromatic rings of **5** and **6** are essentially planar, with a maximal deviation from the least-squares plane of 0.022(3) Å. In **5** the dihedral angles between the aromatic ring planes are small [up to 5(1)°], and the ester COO fragments are almost coplanar with the ring plane. The carbonyl oxygen atoms are *trans* with respect to the nitrogen atoms of the neighbouring pyridine rings, suggesting that weak intramolecular C−H···O=C interactions stabilise this conformation (in a carboxylate group the carbonyl oxygen atom is a better hydrogen bond acceptor than the ester one). In both symmetry-independent molecules the ethoxy fragments on either side of the molecule are differently oriented. This is probably a result of steric interactions between the ethyl groups within the bay region of the molecule. In one of the ethyl groups, the terminal C−C bond is almost coplanar with the main plane of the molecule, while in the other it is almost perpendicular (Figure 1, Table 1).

In **6** the amide groups are essentially planar, but they are more twisted with respect to the respective pyridine ring planes. The twist angles are as large as 58.2(5)° — this may be caused by the steric requirements of four relatively bulky CH_2CH_3 groups. Interestingly, even in this case the carbonyl oxygen atoms are in a *pseudo-trans* orientation with respect to the pyridine nitrogen atom (Table 1). The steric stress is transferred to some extent to the central part of the molecule, and therefore the dihedral angles between the aromatic ring planes are in this case much larger than in **5**, up to 12.02(14)°. The space between the oxygen atoms in the *transoid* conformation of ligand **6** is 8.58 Å.

The bond lengths and angles are unexceptional, and similar in both compounds. The differences between the intraannular bond angles in the terminal pyridine rings can be attributed to the presence of the different substituents.[13] The intraannular angles show a difference between C−C−C and N−C−C angles, the former being about 5°

Table 2. Crystal structures of ligands **5** and **6**; hydrogen bond data [including weak intramolecular C−H···N(O) interactions]

Compound **5**				
D−H···A[a]	D−H (Å)	H···A (Å)	D···A (Å)	D−H···A(θ °)
C(2A)−H(2A)···O(20A)#1	0.93	2.67	3.578(9)	165
C(2B)−H(2B)···O(25B)#1	0.93	2.69	3.604(9)	167
C(11B)−H(11B)···O(20A)#3	0.93	2.54	3.139(7)	123
C(17B)−H(17B)···O(25A)#4	0.93	2.62	3.286(7)	129
C(5A)−H(5A)···N(8A)	0.93	2.54	2.830(8)	99
C(5A)−H(5A)···N(14A)	0.93	2.50	2.814(8)	98
C(18A)−H(18A)···N(3A)	0.93	2.52	2.797(10)	99
C(12A)−H(12A)···N(1A)	0.93	2.45	2.764(9)	100
C(5B)−H(5B)···N(8B)	0.93	2.52	2.778(8)	96
C(5B)−H(5B)···N(14B)	0.93	2.53	2.820(8)	98
C(18B)−H(18B)···N(3B)	0.93	2.43	2.767(9)	102
C(12B)−H(12B)···N(1B)	0.93	2.44	2.743(10)	99
Compound 6				
D−H···A[b]	D−H (Å)	H···A (Å)	D···A (Å)	D−H···A(θ °)
C(23)−H(23C)···O(27)#1	1.03(3)	2.47(3)	3.480(4)	165(2)
C(24)−H(24A)···O(27)#1	0.99(2)	2.63(3)	3.606(3)	168.3(19)
C(29)−H(29A)···O(20)#2	1.04(3)	2.71(3)	3.431(3)	126.5(18)
C(30)−H(30C)···O(20)#2	1.04(4)	2.67(4)	3.337(4)	122(2)
C(31)−H(31A)···O(20)#2	0.99(3)	2.67(3)	3.465(3)	138(2)
C(5)−H(5)···N(8)	0.91(2)	2.51(2)	2.800(3)	99.3(17)
C(5)−H(5)···N(14)	0.91(2)	2.49(2)	2.786(3)	99.6(16)
C(22)−H(22B)···N(14)	1.00(2)	2.74(2)	3.066(3)	99.6(16)
C(23)−H(23B)···N(14)	1.01(3)	2.70(3)	3.318(4)	119(2)
C(18)−H(18)···N(3)	0.94(2)	2.52(2)	2.849(3)	100.5(16)
C(29)−H(29B)···N(8)	1.08(2)	2.26(2)	2.902(3)	116.0(17)
C(30)−H(30B)···N(8)	1.05(3)	2.97(3)	3.380(4)	104(2)

[a] Symmetry transformations used to generate equivalent atoms: #1 $x - 1/2, -y + 1/2, z$; #2 $x + 1/2, -y + 1/2, z$; #3 $x - 1/2, -y - 1/2, z$; #4 $-x + 3/2, y + 1/2, z + 1/2$. [b] Symmetry transformations used to generate equivalent atoms: #1 $-x + 1, -y + 1, -z + 1$; #2 $-x + 1, -y + 1, -z$.

greater than the latter; similar differences have been observed in related compounds.[14]

The crystal packing is governed by van der Waals interactions, weak intermolecular C−H···O(N) interactions (Table 2) and, to some extent, by the π-stacking between the heterocyclic rings.

Synthesis and Characterisation of the Complexes

Multitopic ligands with N,N,O(carbonyl) type donor sets have only infrequently been employed in the metal ion directed assembly of coordination architectures. However, such ligands have been successfully demonstrated to form helicate complexes, in particular with lanthanide metal ions.[3a] The reason for the propensity of the N,N,O (carbonyl) donor set to bind to lanthanides presumably originates from the strong hard-hard, oxygen-lanthanide(III) interaction. The following account describes the successful utilisation of ligands of this type (**5** and **6**) for the generation of [2 × 2] grid architectures with certain first row transition metal ions. Specifically, the syntheses of the new [2 × 2] grid-type complexes **5a**−**c** and **6a**−**c** were performed by reaction of **5** and **6** with iron(II), cobalt(II) and zinc(II) salts (Scheme 2).

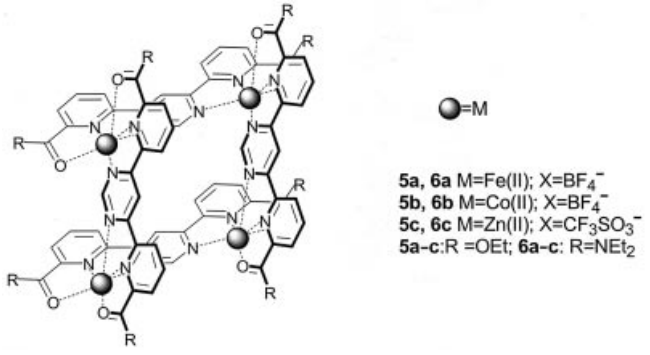

Scheme 2. Schematic representation of the self-assembly of the [2 × 2] grids

The self-assembly of [2 × 2] grid-type compounds was achieved by reaction at room temperature or under reflux in acetonitrile, using the triflate or tetrafluoroborate salt of the corresponding metal ion. The complexation reactions were followed by ESI-MS and NMR spectroscopy. The ^{1}H NMR spectra of the paramagnetic complexes (**5a**, **5b**, **6a**, and **6b**) show strongly shifted signals, as expected, and are strongly supportive of the grid-type structures. In the case of the iron complexes **5a** and **6a**, signals are observed between δ = 88.25 and 1.42 ppm, and δ = 90.96 and −7.79 ppm, respectively, indicating the presence of high-spin iron centres, similar to related grid structures with N,N,N donor sets reported earlier.[15] For the cobalt complexes **5b** and **6b** the signals were found to be shifted to an even greater extent, lying between δ = 130.27 and 1.40 ppm and between δ = 114.33 and −15.23 ppm, respectively. The ^{1}H NMR spectra of the diamagnetic zinc complexes **5c** and **6c** show the signals of a symmetrically coordinated ligand in a single chemical and magnetic environment, in agreement with the grid structure. Interestingly, significant coordination-induced shifts of the signals are observed when the spectra of **5c** and **6c** are compared to those of uncomplexed ligands **5** and **6**.

ESI-MS is a highly sensitive and accurate analytical tool widely used for the characterisation of large, charged biomolecules such as proteins and DNA. The technique has also been found to be particularly successful for the identification of large metallosupramolecular architectures in solution, in which multiply charged ions are generated by sequential loss of counterions, resulting in characteristic isotopic patterns in the spectrum. The ESI-MS investigations of all complexes were performed on acetonitrile solutions at approximately 10^{-4} M. For example, the ESI mass spectrum of **5c** shows peaks corresponding to the multiply charged species: *m/z* = 839.2 (5%, $\{[Zn_4(\mathbf{5})_4](CF_3SO_3)_5\}^{3+}$), 591.0 (100%, $\{[Zn_4(\mathbf{5})_4](CF_3SO_3)_4\}^{4+}$) and 345.2 (5%, $\{[Zn_4(\mathbf{5})_4](CF_3SO_3)_2\}^{6+}$. These data confirm the presence of the grid **5c** in solution. At higher dilutions, significant dissociation of the grid complexes to mononuclear species was found to occur.

The UV/Visible spectrum of complex **6c** in acetonitrile shows an absorption band at around 300 nm. Complex **6c** also affords an intense emission at 372 nm upon excitation at 270 nm at room temperature (Figure 3). The luminescence of this complex may be attributed to emission from the lowest ligand-centred excited singlet level. The absence of emission for the cobalt complex **6b** is due to the presence of the low-lying nonemissive Co^{II}-centred MLCT excited state which inhibits luminescence.[16]

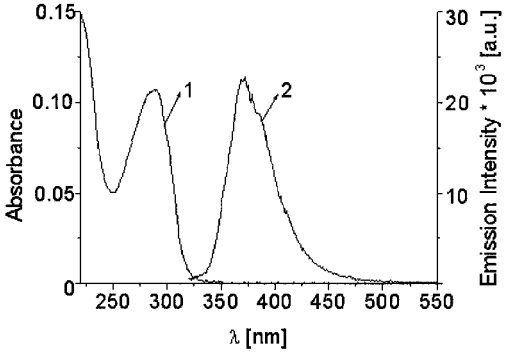

Figure 3. Absorption (1) and emission (2) spectra of $Zn_4L_4(OTf)_8$ complex **6c** at 1×10^{-5} mol/dm^{-3} in CH_3CN solution (λ_{exc} = 270 nm, λ_{em} = 372 nm)

Crystallographic Characterisation of Grid Complexes 6b and 6c

Complexes **6b** and **6c** were crystallographically characterised by X-ray diffraction. The results unambiguously demonstrated the [2 × 2] tetranuclear grid-type structure of the complexes in which the metal ions are hexacoordinated by four nitrogen atoms and the remaining outer positions by oxygen atoms of the carbonyl groups.

Crystal Data for Complex 6b

Crystals of complex **6b** were obtained by diffusion of benzene into a solution of the complex in acetonitrile and its structure was determined by X-ray crystallography (Figure 4 and Table 3). The architecture of this grid is similar to that of the structures of similar compounds.[15,16] The complex **6b** crystallises with two cations per unit cell. The size of this grid is within nanoscopic dimensions, as the intraligand methyl-methyl and pyridine H4-pyridine H4 distances are respectively 15.9−17.9 Å (width) and 9.2−9.4 Å (height). The ligands in the grid are not totally planar but somewhat distorted. The distortion angle varies from 4.4° to 14.5°. There are two anions partially encapsulated inside the cavity of the grid. The size of the cavity is between 6.39 and 6.75 Å. In addition, each anion inside the cavity is surrounded by two molecules of acetonitrile. These molecules of solvent are sandwiched between opposite pyridine moieties. The rest of the anions are positioned between adjacent grids in a layer-like fashion. A limited degree of van der Waals contact between aromatic groups and ethyl chains of adjacent grids is also observed. The Co^{II} ions are situated in a distorted octahedral coordination polyhedron and the Co−Co distances are in the range 6.328−6.395 Å. The Co−N and Co−O bond lengths lie between 2.033 and 2.200 Å and 2.068 and 2.135 Å, respectively.

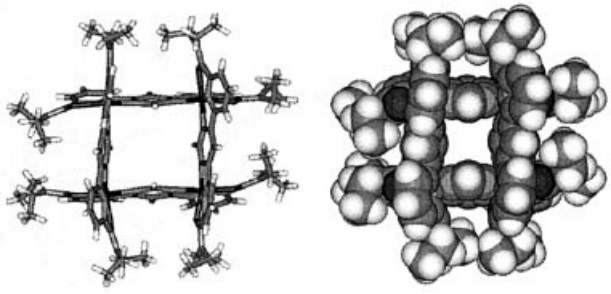

Figure 4. Crystal structure of [2 × 2] grid-type complex **6b**; counterions and solvent molecules are omitted for clarity

Table 3. Selected averaged bond lengths [Å] and angles [°] for complex **6b** (each of the two molecules in the asymmetric unit are presented) and for complex **6c**

Bond/angle[a]	6b	6c
$M-N_{ax}$	2.043 2.043	2.058
$M-N_{eq}$	2.168 2.166	2.170
M−O	2.110 2.106	2.157
$N_{ax}-M-N_{ax}$	163.8 162.4	156.7
$N_{eq}-M-N_{eq}$	95.5 95.9	101.3
O−M−O	100.6 102.2	97.2

[a] M = Co^{II} in **6b** and Zn^{II} in **6c**. ax = M−N bonds to the pyridine moiety, eq = M−N bonds to the pyrimidine moiety.

Crystal Data for Complex 6c

Crystals of complex **6c** were obtained by diffusion of *tert*-butyl methyl ether into a solution of the complex in acetonitrile and its structure was determined by X-ray crystallography (Figure 5 and Table 3). The Zn^{II} ions in complex **6c** also display a distorted octahedral coordination. The Zn−Zn distances are in the range 6.255−6.390 Å. The lengths of the coordinative Zn−N bonds vary from 2.052 to 2.199 Å and the Zn−O bond lengths lie between 2.134 and 2.188 Å. Two CF_3SO_3 ions are partially encapsulated in the cavity of this grid.

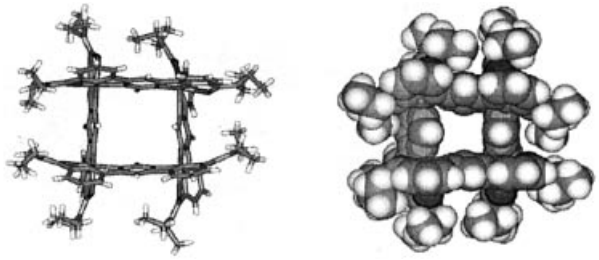

Figure 5. Crystal structure of [2 × 2] grid-type complex **6c**; counterions and solvent molecules are omitted for clarity

Conclusion

The two novel ligands **5** and **6** containing two tridentate N,N,O(carbonyl) binding subunits, have been prepared and their solid-state conformational properties characterised by X-ray crystallography. Reaction of **5** and **6** with Fe^{II}, Co^{II} and Zn^{II} resulted in the clean and quantitative formation of [2 × 2] grid-type complexes, which were characterised in solution on the basis of ESI-MS and ^1H NMR spectroscopy. The structures of the Zn^{II} and Co^{II} complexes **6b** and **6c** were also investigated by X-ray crystallography which confirmed that they were indeed [2 × 2] grid-type architectures with each metal ion octahedrally coordinated by two N,N,O donors. The above work therefore details a particularly facile and rapid synthetic protocol for the preparation of [2 × 2] grid-type coordination scaffolds with first row transition metal ions. Of particular significance is the fact that the N,N,O(carbonyl) donor set approach should enable a wide range of substituents to be externally connected onto the outer surface of the grid. Such substituents may for example be electroactive or mesogenic, or may enable attachment of the complex to gold or graphite surfaces. Many potential future applications may be envisioned for materials of this type, for example, as functional components of molecular electronic devices. These and related avenues of exploration will be reported in due course.

Experimental Section

General: CH_3CN was freshly distilled under argon from CaH_2. 2-Methyl-6-(trimethylstannyl)pyridine (**1**) was prepared according to a literature procedure.[10] The reagents were used as received from Aldrich or Acros without further purification. The NMR spectra were run on a Bruker AC 200 at 200.1 MHz, a Varian Gemini 300, and 500 MHz spectrometer, and were calibrated against residual protonated solvent signal ($CDCl_3$: δ = 7.24 ppm; $[D_6]$DMSO: δ = 2.50 ppm; CD_3CN: δ = 1.94 ppm). Mass spectra were determined by FAB^+ using a ZAB-HF VG apparatus in a *m*-nitrobenzyl alcohol matrix and by ESI-MS using a Waters Micromass ZQ spec-

trometer in acetonitrile. IR spectra were obtained with a Perkin−Elmer 580 spectrophotometer and are reported in cm^{-1}. The electronic absorption spectrum of **6c** was measured on a Shimadzu UV 2401 PC spectrometer in acetonitrile, with λ_{max} in nm and ε ($\times 10^4$) in $M^{-1}cm^{-1}$. The luminescence spectrum for complex **6c** was recorded in CH_3CN using a Perkin−Elmer MPF-3 spectrofluorimeter. Microanalyses were obtained using a Perkin−Elmer 2400 CHN microanalyzer. Melting points were recorded on an Electrothermal Digital melting point apparatus.

4,6-Bis[6-(2-methylpyridyl)]pyrimidine (2): 2-Methyl-6-(trimethylstannyl)pyridine (**1**; 5 g, 20 mmol) and degassed toluene (45 mL) were added consecutively by syringe to a mixture of 4,6-dichloropyrimidine (0.9818 g, 6 mmol), $Pd(PPh_3)_4$ (0.27 g, 0.9 mmol) and LiCl (1.7 g, 29 mmol) under an argon atmosphere. The reaction was refluxed and stirred at 120 °C for 24 h, and the toluene was then evaporated on a water bath under reduced pressure. The residue was purified by column chromatography on alumina, eluting with dichloromethane, to afford 1.547 g (90%) **2**. ^1H NMR (400 MHz, $CDCl_3$): δ = 9.32 (s, 1 H, H2), 9.30 (s, 1 H, H5), 8.26 (d′, *J* = 5.49 Hz, 2 H, H5′, -5′), 7.75 (t, *J* = 5.95 Hz, 2 H, H4′, -4′′), 7.28 (d, *J* = 5.19 Hz, 2 H, H3′, -3′′), 2.75 (s, CH_3) ppm. ^{13}C NMR (75 MHz, $CDCl_3$): δ = 164.07, 158.46, 158.34, 153.49, 136.98, 124.78, 118.77, 113.85, 24.70 ppm. FAB-MS: *m*/*z* (%) = 263.0 (100) [**2** + H]. IR (KBr): ṽ = 3408, 2917, 1597, 1571, 1530, 1448, 1379, 1228, 1158, 1090, 989, 904, 808, 771, 640, 438 cm^{-1}. $C_{16}H_{14}N_4$ (262.31): calcd. C 73.26, H 5.38, N 21.36; found C 73.04, H 5.46, N 21.24. M.p. 126−128 °C.

2,2′-Bis(4,6-pyrimidinediyl)pyridine-6,6′-dicarboxylic Acid (3): Product **2** (0.35 g, 1.3 mmol) was added to concentrated H_2SO_4 (10 mL) and cooled to 0 °C with stirring in an ice-bath. Chromium(VI) oxide (0.80 g, 8 mmol) was then added in 0.1 g portions to the stirred solution of **2** at a rate that maintained the reaction temperature below 3 °C. When the addition of CrO_3 was completed (about 5 h) the mixture was stirred for 9 hours at 0−5 °C, and 42 hours at room temperature. The viscous reaction solution was then poured onto excess crushed ice with stirring. The precipitated product was finally isolated by filtration under reduced pressure, washed with distilled water and air dried to yield 0.348 g (81%) of **3**. ^1H NMR (200 MHz, DMSO): δ = 9.50 (s, 1 H, H2), 9.35 (s, 1 H, H5), 8.72 (t′, *J* = 4.75 Hz, 2 H, H4′, -4′), 8.27 (d, *J* = 4.57 Hz, 4 H, H3′, -3′′, -5′, -5′′) ppm. IR (KBr): ṽ = 3411, 2926, 1746, 1646, 1581, 1533, 1452, 1367, 1252, 1168, 1086, 995, 905, 838, 752, 636, 607, 471, 427 cm^{-1}. $C_{16}H_{10}N_4O_4{\cdot}2H_2O$ (358.31): calcd. C 53.63, H 3.91, N 15.64; found C 53.25, H 3.70, N 15.03. M.p. 253 °C

2,2′-Bis(4,6-pyrimidinediyl)pyridine-6,6′-dicarboxylic Acid Chloride (4): Compound **3** (0.133 g, 0.4 mmol) was refluxed for 5 h in thionyl chloride (20 mL) and then the $SOCl_2$ evaporated under reduced pressure on a water bath. The crude **4** was then used immediately for the subsequent synthesis of diester **5** and diamide **6** without further purification.

Diethyl 2,2′-Bis(4,6-pyrimidinediyl)pyridine-6,6′-dicarboxylate (5): EtOH (20 mL) was added to **4** (0.148 g, 0.41 mmol) and the resulting mixture refluxed for 15 h and subsequently cooled to room temperature. The reaction was then reduced in volume to 8 mL under pressure on a water bath, and the mixture cooled in an ice-bath. The crystalline solid was isolated by filtration under vacuum, washed with a small quantity of ice-cold EtOH and air dried to yield 0.138 g (88%) **5** as white needles. ^1H NMR (300 MHz, $CDCl_3$): δ = 9.51 (s, 1 H, H2), 9.38 (s, 1 H, H5), 8.70 (d, *J* = 8.1 Hz, 2 H, H5′, -5′′), 8.24 (d, *J* = 7.8 Hz, 2 H, H3′, -3′′), 8.05 (t, *J* = 7.8 Hz, 2 H, H4, -4′), 4.52 (q, *J* = 6.9 Hz, 4 H, CH_2), 1.51 (t, *J* = 7.2 Hz, 6 H, CH_3) ppm. ^{13}C NMR (DEPT, 75 MHz, $CDCl_3$): δ = 165.16, 163.57, 158.55 (CH), 154.51, 148.70, 138.09 (CH), 126.40 (CH), 124.84 (CH), 115.05 (CH), 61.95 (CH_2), 14.29 (CH_3) ppm. FAB-MS: *m*/*z* (%) = 379.4 (100) [**5** + H]. IR (KBr): ṽ = 3410, 2982, 1715, 1646, 1575, 1529, 1447, 1318, 1259, 1150, 1083, 992, 919, 838, 756, 701, 636, 471, 433 cm^{-1}. $C_{20}H_{18}N_4O_4$ (378.39): calcd. C 63.49, H 4.79, N 14.81; found C 63.17, H 4.82, N 14.44. M.p. 162 °C.

2,2′-Bis(4,6-pyrimidinediyl)pyridine-6,6′-diethyl Diamide (6): Anhydrous THF (5 mL), and a solution of Et_2NH (10 mL) in anhydrous THF (50 mL) were added consecutively by syringe to **4** (0.2592 g, 0.72 mmol) under an atmosphere of argon. The resulting mixture (pale brown suspended solid) was then stirred for 20 h at ambient temperature, and filtered under gravity. The filtrate was evaporated to dryness and the remaining solid dissolved in boiling *n*-hexane (100 mL), filtered under gravity, and left to stand overnight. The crystalline solid which formed was isolated by filtration under vacuum, washed with ice-cold hexane and air dried to yield 0.118 g (38%) **6** as white needles. ^1H NMR (300 MHz, $CDCl_3$): δ = 9.37 (s, 2 H, H2, H5), 8.58 (d, *J* = 7.8 Hz, 2 H, H5′, -5′′), 8.00 (t′, *J* = 7.8 Hz, 2 H, H4′, -4′), 7.79 (d′, *J* = 7.8 Hz, 2 H, H3′, -3′), 3.62 (q, *J* = 7.2 Hz, 4 H, CH_2), 3.47 (q, *J* = 7.2 Hz, 4 H, CH_2), 1.33 (t, *J* = 6.9 Hz, 6 H, CH_3), 1.29 (t, *J* = 7.2 Hz, 6 H, CH_3) ppm. ^{13}C NMR (DEPT, 75 MHz, $CDCl_3$): δ = 167.70, 163.42, 158.36 (CH), 154.83, 152.42, 137.60 (CH), 125.05 (CH), 122.04 (CH), 113.93 (CH), 43.48 (CH_2), 40.52 (CH_2), 14.69 (CH_3), 13.01 (CH_3) ppm. FAB-MS: *m*/*z* (%) = 433.2 (100) [**6** + H]. IR (KBr): ṽ = 3412, 2975, 1636, 1569, 1477, 1443, 1377, 1316, 1117, 1080, 993, 827, 756, 636, 608, 472, 409 cm^{-1}. $C_{24}H_{28}N_6O_2$ (432.53): calcd. C 66.58, H 6.52, N 19.43; found C 66.39, H 6.42, N 18.50. M.p. 123 °C.

Fe Complex (5a): An equimolar mixture of $Fe(BF_4)_2{\cdot}6H_2O$ (9.8 mg, 29 μmol) and ligand **5** (11.0 mg, 29 μmol) in MeCN (5 mL) was stirred at room temperature for 10 h. The solvent was evaporated under reduced pressure to give a quantitative yield of **5a** as a blue powder. ^1H NMR (300 MHz, CD_3CN): δ = 88.25, 64.59, 34.53, 31.15, 9.36 (d), 8.75, 8.75, 8.27, 4.47, 3.75, 2.57, 1.42 ppm. IR (KBr): ṽ = 3349, 2991, 1635, 1577, 1533, 1444, 1381, 1247, 1219, 1033, 929, 875, 795, 755, 703, 657, 581, 417 cm^{-1}. $Fe_4(\mathbf{5})_4(BF_4)_8$ (2469.34): calcd. C 38.91, H 2.44, N 9.08; found C 39.21, H 2.53, N 9.78.

Co Complex (5b): A solution of ligand **5** (10.0 mg, 26 μmol) and $Co(BF_4)_2{\cdot}6H_2O$ (9.0 mg, 26 μmol) in MeCN (5 mL) was heated under reflux for 10 h. The red complex **5b** was isolated in quantitative yield by evaporation of the solvent. ESI-MS: *m*/*z* = 1135 $\{[Co_4(\mathbf{5})_4](BF_4)_6\}^{2+}$, 218 $\{[Co_4(\mathbf{5})_4]\}^{8+}$. ^1H NMR (300 MHz, CD_3CN): δ = 130.27, 100.79, 97.26, 87.88, 72.57, 68.41, 62.20, 34.07, 14.48, 11.42, 9.49 (d), 8.75, 8.27, 8.04, 6.56, 5.98, 4.45, 3.56, 2.95, 1.76, 1.42, 1.40 ppm. IR (KBr): ṽ = 3371, 3084, 1613, 1573, 1531, 1442, 1385, 1265, 1212, 1158, 1034, 928, 878, 794, 759, 701, 672, 657, 587, 444 cm^{-1}. $Co_4(\mathbf{5})_4(BF_4)_8$ (2481.69): calcd. C 38.72, H 2.92, N 9.03; found C 39.07, H 2.98, N 9.65.

Zn Complex (5c): An equimolar mixture of $Zn(CF_3SO_3)_2$ (9.6 mg, 26 μmol) and ligand **5** (10.0 mg, 26 μmol) in MeCN (5 mL) was stirred at room temperature for 22 h. The solvent was evaporated under reduced pressure to yield the dark yellow complex **5c** in quantitative yield. ESI-MS: *m*/*z* = 839.2 $\{[Zn_4(\mathbf{5})_4](CF_3SO_3)_5\}^{3+}$, 591.0 $\{[Zn_4(\mathbf{5})_4](CF_3SO_3)_4\}^{4+}$, 345.2 $\{[Zn_4(\mathbf{5})_4](CF_3SO_3)_2\}^{6+}$. ^1H NMR (300 MHz, CD_3CN): δ = 9.71 (s), 9.57 (d), 9.36 (s), 8.70 (d), 8.33 (t), 4.50 (m), 1.71 (t, *J* = 5.1 Hz) ppm. IR (KBr): ṽ = 3452, 3095, 1724, 1693, 1620, 1582, 1538, 1475, 1452, 1404, 1381, 1342, 1263, 1163, 1100, 1031, 857, 840, 758, 723, 704, 638, 574, 518, 446,

405 cm^{-1}. $Zn_4(\mathbf{5})_4(CF_3SO_3)_8$ (2967.65): calcd. C 35.62, H 2.45, N 7.55; found C 36.12, H 2.44, N 7.07.

Fe Complex (6a): An equimolar mixture of $Fe(BF_4)_2{\cdot}6H_2O$ (5.5 mg, 16 μmol) and ligand **6** (7.1 mg, 16 μmol) in MeCN (4 mL) was stirred at room temperature for 16 h. The solvent was evaporated under reduced pressure to give a quantitative yield of **6a** as a blue powder. ESI-MS: *m*/*z* = 1236.9 $\{[Fe_4(\mathbf{6})_4](BF_4)_6\}^{2+}$, 291.1 $\{[Fe_4(\mathbf{6})_4](BF_4)\}^{7+}$. ^{1}H NMR (200 MHz, CD_3CN): δ = 90.96, 87.54, 74.31, 63.69, 48.69, 32.52, 29.96, 27.64, 18.19, 16.91, 14.04, 12.03, 9.89, 7.64, 5.32, 3.98, 0.07, −4.80, −5.54, −7.79 ppm. IR (KBr): $\tilde{\nu}$ = 3403, 2926, 2854, 1632, 1570, 1530, 1485, 1447, 1379, 1363, 1299, 1259, 1221, 1182, 1120, 1084, 1071, 1042, 993, 827, 810, 756, 640, 574, 533, 522 cm^{-1}. $Fe_4(\mathbf{6})_4(BF_4)_8$ (2647.89): calcd. C 43.55, H 4.26, N 12.70; found C 40.36, H 4.03, N 12.53.

Co Complex (6b): A solution of ligand **6** (14.8 mg, 34 μmol) and $Co(BF_4)_2{\cdot}6H_2O$ (11.7 mg, 34μmol) in MeCN (7 mL) was heated under reflux for 19 h. The red complex **6b** was isolated in quantitative yield upon evaporation of the solvent. ESI-MS: *m*/*z* = 799.9 $\{[Co_4(\mathbf{6})_4](BF_4)_5\}^{3+}$, 578.1 $\{[Co_4(\mathbf{6})_4](BF_4)_4\}^{4+}$, 356 $\{[Co_4(\mathbf{6})_4](BF_4)_2\}^{6+}$. ^{1}H NMR (200 MHz, CD_3CN): δ = 114.33, 71.57, 21.68, 14.66, 10.51, 6.30, 5.45, 4.72, −2.11, −4.31, −10.13, −13.40, −15.23 ppm. IR (KBr): $\tilde{\nu}$ = 3439, 2978, 2931, 1719, 1636, 1609, 1572, 1534, 1485, 1442, 1386, 1363, 1266, 1208, 1083, 1033, 827, 756, 657, 522 cm^{-1}. $Co_4(\mathbf{6})_4(BF_4)_8$ (2660.24): calcd. C 43.34, H 4.24, N 12.64; found C 46.95, H 4.31, N 11.84.

Zn Complex (6c): A solution of ligand **6** (6.2 mg, 14 μmol) and $Zn(CF_3SO_3)_2$ (5.2 mg, 14μmol) in MeCN (3 mL) was stirred at room temperature for 19 h. The pale yellow complex **6c** was isolated in quantitative yield upon evaporation of the solvent. ^{1}H NMR (300 MHz, CD_3CN): δ = 9.70 (s), 9.42(s), 9.23 (d, *J* = 7.8 Hz), 8.68 (t, *J* = 7.8 Hz), 8.29 (d, *J* = 7.8 Hz), 3.48 (q), 3.12 (q, *J* = 6.3 Hz), 1.32 (t, *J* = 6.9 Hz) ppm. IR (KBr): $\tilde{\nu}$ = 3441, 2981, 1613, 1533, 1487, 1461, 1377, 1364, 1279, 1259, 1224, 1159, 1031, 993, 829, 757, 638, 574, 517 cm^{-1}. $Zn_4(\mathbf{6})_4(CF_3SO_3)_8{\cdot}10CH_3CN{\cdot}H_2O$ (3612.72): calcd. C 41.22, H 4.02, N 13.18; found C 44.01, H 4.30, N 12.21. UV/Vis: 298.0 (1.1).

Crystal Structure Determination of Ligands 5 and 6: Colourless crystals of dimensions 0.05 × 0.1 × 0.5 mm (compound **5**) and 0.2 × 0.25 × 0.25 mm (compound **6**) were chosen for X-ray data collection (see also Table 4). For ligand **5**, diffraction data were collected at room temperature by the ω-scan technique up to 2Θ = 40°, on a KUMA KM4CCD four-circle diffractometer with graphite-monochromated Mo-K_α radiation (λ = 0.71073Å). For ligand **6**, the data collection was performed with KUMA KM4 κ-geometry diffractometer equipped with point detector, using graphite-monochromated Cu-K_α radiation (λ = 1.54178Å) and ω-2θ scan method. All data were corrected for Lorentz-polarisation effects. The structures were solved with direct methods with SHELXS-97[17] and refined by full-matrix least-squares procedures on F^2 with SHELXL-97.[17] All non-hydrogen atoms were refined anisotropically, for **5** hydrogen atoms were located at calculated positions and refined as a ''riding model' with isotropic thermal parameters fixed at 1.2-times the U_{eq}'s of appropriate carrier atom, while for **6** both positional and thermal parameters of hydrogen atoms were refined.

Table 4. Crystallographic data for the structural analyses of ligands **5** and **6**

	5	**6**
Empirical formula	$C_{20}H_{16}N_4O_4$	$C_{24}H_{28}N_6O_2$
Molecular weight	376.7	432.5
a (Å)	18.675(3)	10.457(5)
b (Å)	4.3936(13)	10.713(3)
c (Å)	44.604(5)	11.242(3)
α (°)	90	86.98(2)
β (°)	90	77.11(3)
γ (°)	90	67.49(3)
V (Å^3)	3659.8(13)	1133.4(5)
Z	8	2
Space group	$Pna2_1$ (No. 33)	$P\bar{1}$ (No.2)
D_{calc} (g·cm^{-3})	1.37	1.27
μ(Mo-K_α) (mm^{-1})	0.10	0.67
$R(F)$ [$F^2 > 2\sigma(F^2)$][a]	0.0508	0.0445
$R_w(F^2)$ [all data][b]	0.0876	0.1209

[a] $R(F) = \Sigma||F_o| - |F_c||/\Sigma|F_o|$. [b] $Rw(F^2) = (\Sigma[w(F_o^2 - F_c^2)^2/\Sigma[w(F_o^2)^2])^{1/2}$.

Table 5. Crystallographic data for the structural analyses of complexes **6b** and **6c**

	6b	**6c**
Empirical formula	$2[C_{96}H_{112}O_8N_{24}Co_4]^{8+}{\cdot}16BF_4^-{\cdot}14.5CH_3CN{\cdot}8C_6H_6{\cdot}H_2O$	$[C_{96}H_{112}O_8N_{24}Zn_4]^{8+}{\cdot}8CF_3SO_3^-{\cdot}5CH_3CN{\cdot}4C_6H_6{\cdot}H_2O$
Molecular weight	6553.66	3405.41
a (Å)	23.2752(2)	18.3628(1)
b (Å)	26.7290(2)	20.6511(2)
c (Å)	27.1194(3)	23.0437(2)
α (°)	77.0095(3)	108.0590(3)
β (°)	85.0779(3)	112.4300(4)
γ (°)	74.7044(6)	95.6630(3)
V (Å^3)	15851.2(3)	7441.7(1)
Z	2	2
Space group	$P\bar{1}$ (No.2)	$P\bar{1}$ (No. 2)
D_{calc} (g·cm^{-3})	1.373	1.520
μ(Mo-K_α) (mm^{-1})	0.512	0.859
$R(F)$ [$F^2 > 2\sigma(F^2)$][a]	0.0918	0.0816
$R_w(F^2)$ [all data][b]	0.2515	0.2256

[a] $R(F) = \Sigma||F_o| - |F_c||/\Sigma|F_o|$for 28779 and 15857 observed reflections for **6b** and **6c**, respectively. [b] $Rw(F^2) = (\Sigma[w(F_o^2 - F_c^2)^2/\Sigma[w(F_o^2)^2])^{1/2}$.

Compound **5** crystallises with two molecules in the asymmetric part of the unit cell. A normal probability plot shows that the differences in geometrical parameters between these two symmetry-independent molecules are of a statistical nature.

Crystal Structure Determination of Complexes 6b and 6c: A summary of crystal data and refinement parameters is given in Table 5. Data were collected on a Nonius Kappa CCD diffractometer at 173.0 ± 0.1 K using graphite-monochromated Mo-K_α radiation (λ = 0.71073 Å). The CCD data were processed with Denzo-SMN v0.95.373.[18] Corrections for Lorentz and polarisation effects were applied. The structures were solved by Patterson method (SHELXS-97)[17] and refined on F^2 by full-matrix least-squares techniques (SHELXL-97).[17] Empirical absorption correction from multiple reflections was performed for both data (Platon for Windows).[19] Scattering factors, corrected for anomalous dispersion, were used as implemented in the refinement program.

The asymmetric unit of complex **6b** contains two of each species. Of 150268 measured reflections in the range 2.10−50.04° in 2θ (and ω scans), 54918 were unique (R_{int} = 0.1215). A red 0.20 × 0.20 × 0.40 mm block-shaped crystal of $2[C_{96}H_{112}Co_4N_{24}O_8]^{8+}\cdot 16BF_4^-\cdot 14.5CH_3CN\cdot 8C_6H_6\cdot H_2O$ was used for data collection. Minimum and maximum transmission factors of 0.758/0.824. All non-hydrogen atoms were refined with anisotropic displacement parameters, except for seven anions, five acetonitriles, a benzene molecule and a water molecule, which were refined isotropically owing to large thermal movement and disorder. Thirteen anions, two acetonitriles, the water molecule and carbon C23H of one of the grids are disordered over two positions. One acetonitrile molecule was refined with population parameter 0.5. A bond restraint in the C−N bond of the disordered part of the grid had to be used to keep the disorder model chemically reasonable. Hydrogen atoms were calculated to their idealised positions with isotropic temperature factors (1.2- or 1.5-times C temperature factor) and refined as riding atoms. No hydrogen atoms were determined for water and one of the disordered acetonitriles. Final agreement factors were obtained for 3865 parameters and one restraint; GOF 1.023. The largest peak and hole in the final difference map were 1.257 and −0.945 e·Å^{-3} and are located near disordered benzene and disordered anion.

A pale yellow 0.20 × 0.30 × 0.30 mm block-shaped crystal of $[C_{96}H_{112}O_8N_{24}Zn_4]^{8+}\cdot 8CF_3SO_3^-\cdot 5CH_3CN\cdot 4C_6H_6\cdot H_2O$ was used for data collection. Of 67176 measured reflections in the range 2.34−50.02° in 2θ (and ω scans), 25963 were unique (R_{int} = 0.0713). Minimum and maximum transmission factors of 0.646/0.710. All non-hydrogen atoms were refined with anisotropic displacement parameters, except for five anions, which were refined partly isotropically owing to large thermal movement and disorder. Two acetonitrile molecules were refined with population parameter 0.5. Five anions and two methyl carbons (C22B and C24) of the grid are disordered over two positions. Temperature factor of disordered methyl C22F was equalised with C22B. Hydrogen atoms were calculated to their idealised positions with isotropic temperature factors (1.2- or 1.5-times C temperature factor) and refined as riding atoms. No hydrogen atoms were determined for water. Final agreement factors were obtained for 1898 parameters; GOF 1.027. The largest peak and hole in the final difference map were 1.330 and −1.100 e·Å^{-3} and are located near one of the disordered anions.

CCDC-205374 (**5**), -205375 (**6**), -205462 (**6b**) and -205463 (**6c**). contain the supplementary crystallographic data for this paper. These data can be obtained free of charge at www.ccdc.cam.ac.uk/conts/retrieving.html [or from the Cambridge Crystallographic Data Centre, 12, Union Road, Cambridge CB2 1EZ, UK; Fax: (internat.) +44-1223/336-033; E-mail: deposit@ccdc.cam.ac.uk].

Acknowledgments

We thank NATO for postdoctoral fellowship to V. P. We also thank Dr. Zbigniew Hnatejko for absorption and fluorescence measurements. This work was partly supported by the Polish State Committee for Scientific Research (grant no. 4 T09A 049 24).

[1] [1a] J.-M. Lehn, *Angew. Chem. Int. Ed. Engl.* **1990**, *29*, 1304−1319. [1b] J.-M. Lehn, *Supramolecular Chemistry-Concepts and Perspectives*, VCH, Weinheim, **1995**.

[2] [2a] J. S. Lindsey, *New J. Chem.* **1991**, *15*, 153−180. [2b] P. Molenveld, J. F. J. Engbersen, D. N. Reinhoudt, *Chem. Soc. Rev.* **2000**, *29*, 75−86. [2c] S. Leininger, B. Olenyuk, P. J. Stang, *Chem. Rev.* **2000**, *100*, 853−908. [2d] G. F. Swiegers, T. J. Malefetse, *Chem. Rev.* **2000**, *100*, 3483−3537. [2e] L. M. Greig, D. Philp, *Chem. Soc. Rev.* **2001**, *30*, 287−302. [2f] C. V. K. Sharma, *J. Chem. Ed.* **2001**, *78*, 617−622.

[3] [3a] C. Piguet, G. Bernardinelli, G. Hopfgartner, *Chem. Rev.* **1997**, *97*, 2005−2062. [3b] M. Albrecht, *Chem. Rev.* **2001**, *101*, 3457−3497. [3c] R. Krämer, J.-M. Lehn, A. Marquis-Rigault, *Proc. Natl. Acad. Sci. USA* **1993**, *90*, 5394−5398. [3d] E. C. Constable, *Tetrahedron* **1992**, *48*, 10013−10059.

[4] [4a] P. N. W. Baxter, H. Sleiman, J.-M. Lehn, K. Rissanen, *Angew. Chem. Int. Ed. Engl.* **1997**, *36*, 1294−1296. [4b] H. Sleiman, P. N. W. Baxter, J.-M. Lehn, K. Airola, K. Rissanen, *Inorg. Chem.* **1997**, *36*, 4734−4742. [4c] M. C. Jimenez-Molero, Ch. Dietrich-Buchecker, J.-P. Sauvage, *Chem. Eur. J.* **2002**, *8*, 1455−1466.

[5] [5a] D. Freedman, S. Sayan, T. J. Emge, M. Croft, J. G. Brennan, *J. Am. Chem. Soc.* **1999**, *121*, 11713−11719. [5b] J. Xu, K. N. Raymond, *Angew. Chem. Int. Ed.* **2000**, *39*, 2745−2747. [5c] B. K. Roland, H. D. Selby, M. D. Carducci, Z. Zheng, *J. Am. Chem. Soc.* **2002**, *124*, 3222−3223. [5d] R. W. Saalfrank, U. Reimann, M. Göritz, F. Hampel, A. Scheurer, F. W. Heinemann, M. Büschel, J. Daub, V. Schünemann, A. X. Trautwein, *Chem. Eur. J.* **2002**, *8*, 3614−3619.

[6] [6a] M. Fujita, Y. J. Kwon, O. Sasaki, K. Yamaguchi, K. Ogura, *J. Am. Chem. Soc.* **1995**, *117*, 7287−7288. [6b] R. L. Paul, S. M. Couchman, J. C. Jeffery, J. A. McCleverty, Z. R. Reeves, M. D. Ward, *J. Chem. Soc., Dalton Trans.* **2000**, 845−851.

[7] [7a] A. M. Garcia, D. M. Bassani, J.-M. Lehn, G. Baum, D. Fenske, *Chem. Eur. J.* **1999**, *5*, 1234−1238. [7b] M. Yoshizawa, T. Kusukawa, M. Fujita, S. Sakamoto, K. Yamaguchi, *J. Am. Chem. Soc.* **2001**, *123*, 10454−10459. [7c] M. Yoshizawa, Y. Takeyama, T. Kusukawa, M. Fujita, *Angew. Chem. Int. Ed.* **2002**, *41*, 1347−1349.

[8] For example: [8a] M.-T. Youinou, N. Rahmouni, J. Fischer, J. A. Osborn, *Angew. Chem. Int. Ed. Engl.* **1992**, *31*, 733−735. [8b] P. N. W. Baxter, G. S. Hanan, J.-M. Lehn, *Chem. Commun.* **1996**, 2019−2020. [8c] M. Fujita, Y. J. Kwon, S. Washizu, K. Ogura, *J. Am. Chem. Soc.* **1994**, *116*, 1151−1152. [8d] P. N. W. Baxter, J.-M. Lehn, B. Kneisel, D. Fenske, *Chem. Commun.* **1997**, 2231−2232. [8e] J. Rojo, M. Ruben, E. Breuning, J.-P. Giesselbrecht, J.-M. Lehn, *Angew. Chem. Int. Ed.* **2000**, *39*, 4139−4142. [8f] G. S. Hanan, D. Volkmer, U. S. Schubert, J.-M. Lehn, G. Baum, D. Fenske, *Angew. Chem. Int. Ed. Engl.* **1997**, *36*, 1842−1844. [8g] O. Waldmann, J. Hassmann, P. Müller, G. S. Hanan, D. Volkmer, U. S. Schubert, J.-M. Lehn, *Physical Rev. Lett.* **1997**, *17*, 3390−3393. [8h] J. Rojo, J.-M. Lehn, G. Baum, D. Fenske, O. Waldmann, P. Müller, *Eur. J. Inorg. Chem.* **1999**, 517−522. [8i] E. Breuning, M. Ruben, J.-M. Lehn, F. Renz, Y. Garcia, V. Ksenofontov, P. Gütlich, E. Wegelius, K. Rissanen, *Angew. Chem. Int. Ed.* **2000**, *39*, 2504−2505.

[8j] H. Oshio, H. Onodera, O. Tamada, H. Mizutani, T. Hikichi, T. Ito, *Chem. Eur. J.* **2000**, 2523−2530. [8k] P. N. W. Baxter, J.-M. Lehn, K. Rissanen, *Chem. Commun.* **1997**, 1323−1324. [8l] P. N. W. Baxter, R. G. Khoury, J.-M. Lehn, G. Baum, D. Fenske, *Chem. Eur. J.* **2000**, *6*, 4140−4148. [8m] A. Marquis, J.-P. Kintzinger, R. Graff, P. N. W. Baxter, J.-M. Lehn, *Angew. Chem. Int. Ed.* **2002**, *41*, 2760−2764. [8n] J. P. Plante, P. D. Jones, D. R. Powell, T. E. Glass, *Chem. Commun.* **2003**, 336−337. [8o] M. Ruben, E. Breuning, M. Barboiu, J.-P. Gisselbrecht, J.-M. Lehn, *Chem. Eur. J.* **2003**, *9*, 291−299.

[9] J. Park, A. N. Pasupathy, J. I. Goldsmith, C. Chang, Y. Yaish, J. R. Petta, M. Rinkoski, J. P. Sethna, H. D. Abruña, P. L. McEuen, D. C. Ralph, *Nature* **2002**, *417*, 722−725.

[10] [10a] P. Jutzi, U. J. Gilge, *Organomet. Chem.* **1983**, *246*, 163. [10b] G. V. Long, S. E. Boyd, M. M. Harding, I. E. Buys, T. W. Hambley, *J. Chem. Soc., Dalton Trans.* **1993**, 3175−3180.

[11] J. K. Stille, *Angew. Chem. Int. Ed. Engl.* **1986**, *25*, 508−524.

[12] G. S. Hannan, J.-M. Lehn, N. Kyritsakas, J. Fischer, *J. Chem. Soc., Chem. Commun.* **1995**, 765−766; D. M. Bassani, J.-M. Lehn, G. Baum, D. Fenske, *Angew. Chem. Int. Ed. Engl.* **1997**, *36*, 1845−1847; D. M. Bassani, J.-M. Lehn, *Bull. Soc. Chim. Fr.* **1997**, *134*, 897−906; M. Ohkita, J.-M. Lehn, G. Baum, D. Fenske, *Chem. Eur. J.* **1999**, *12*, 3471−3481.

[13] A. Domenicano, P. Murray-Rust, *Tetrahedron Lett.* **1979**, *24*, 2283−2286.

[14] G. S. Hanan, U. S. Schubert, D. Volkmer, E. Rivière, J.-M. Lehn, N. Kyritsakas, J. Fischer, *Can. J. Chem.* **1997**, *75*, 169−182.

[15] E. Breuning, U. Ziener, J.-M. Lehn, E. Wegelius, K. Rissanen, *Eur. J. Inorg. Chem.* **2001**, 1515−1521.

[16] J. Rojo, F. J. Romero-Salguero, J.-M. Lehn, G. Baum, D. Fenske, *Eur. J. Inorg. Chem.* **1999**, 1421−1428.

[17] SHELX97 − Programs for Crystal Structure Analysis (Release 97−2). Sheldrick, G. M., Institüt für Anorganische Chemie der Universität, Tammanstrasse 4, 3400 Göttingen, Germany, **1998**.

[18] Z. Otwinowski, W. Minor, "Processing of X-ray Diffraction Data Collected in Oscillation Mode", Methods in Enzymology, Volume 276: Macromolecular Crystallography, part A, p. 307−326, **1997**, C. W. Carter, Jr. & R. M. Sweet, Eds., Academic Press.

[19] R. H. Blessing, *Acta Crystallogr., Sect. A* **1995**, *51*, 33−38; PLATON, A Multipurpose Crystallographic Tool, Utrecht University, Utrecht, The Netherlands, Spek, A. L. **1998**.

Received May 26, 2003
Early View Article
Published Online October 2, 2003

